



Controlling chaos for energy harvesting via digital extended time-delay feedback

José Geraldo Telles Ribeiro^{1,a} , Marcelo Pereira^{1,2,b} , Americo Cunha Jr^{1,c} , and Lisandro Lovisolo^{1,d}

¹ Rio de Janeiro State University – UERJ, Rio de Janeiro, Brazil

² SENAI Innovation Institute for Virtual Production Systems (Firjan SENAI), Rio de Janeiro, Brazil

Received 25 September 2021 / Accepted 20 February 2022 / Published online 3 March 2022

© The Author(s), under exclusive licence to EDP Sciences, Springer-Verlag GmbH Germany, part of Springer Nature 2022

Abstract Chaotic vibrations may appear in nonlinear energy harvesting systems, which can be problematic when using the recovered power, as it may require an extra expenditure of energy to rectify the voltage signal or reduce the harvesting process efficiency when charging the battery. Both cases can derail the energy harvester's functionality. An alternative in this situation is to explore chaos control to stabilize the system dynamics so that the recovered voltage signal is regular and more suitable for use in the applications of interest. This paper address this problem employing an extended delayed feedback method that combines a displacement actuator and a digital controller to implement the control mechanism. The control strategy is mathematically formulated and tested in a bistable energy harvesting system that often operates in a chaotic regime. The controller shows itself capable of stabilizing the chaotic dynamics at a very low energetic cost.

1 Introduction

Energy harvesting is a process of converting energy available for free in the environment into electrical power for use in small electronic components, that may be used in wireless sensors, bio-implants, etc. This technology is capable of obtaining electrical energy from kinetic, thermal, solar energy sources, etc [1,2], which enables it as a potential replacement for batteries, which are intrinsically limited (requires periodic replacement or recharging) and polluting (toxic and very short life).

Vibration energy harvesters with linear structural dynamics present an important limitation since if the excitation frequency deviates slightly from the fundamental resonance frequency of the energy harvester, the electrical power output is drastically reduced. This limitation can be avoided through the use of geometric nonlinearities, that induce high-amplitude oscillations even far from a resonance frequency, increasing in this way the frequency band where it is possible to recover “large” amounts of power [3–10].

A typical prototype for a vibration nonlinear energy harvester that explores this idea is illustrated in Fig. 1a, it is a bistable electromechanical oscillator, capable of vibrating at high amplitudes, which can therefore recover energy in a wide frequency band. This system

uses piezoelectric plates bonded to a long cantilever beam to harvest energy from the ambient vibration. In this mechanism the inertial excitation from the moving base imposes a deflection in the beam which, consequently, generates an electric tension in the piezoelectric material [11–16]. Applications of this kind of technology can be seen in the wings of a UAV [17,18] and for jet engine monitoring [19], etc.

Although nonlinearity may be beneficial for this system, as it significantly expands the frequency range where the system can operate, it can also bring an inconvenience if it starts to vibrate in a chaotic regime. In this case, the rectification process of the voltage signal generated in the piezoelectric transducer can demand a considerable part of the available energy or the charging time of the storage battery can be very long, situations that can make the practical use of the harvester unfeasible [20].

A very appealing alternative in this scenario is to exploit chaos control techniques [21] to stabilize chaotic dynamics with minimal energy expenditure, so that the energy harvesting device does not lose its functionality. Some works in this direction have already been reported in recent literature, exploring the classical OGY discrete technique [22,23], as well as a continuous extended feedback approach [24]. Despite showing that chaos control can be promising in energy harvesting, none of these works explore a digital architecture for chaos control, which is indispensable for these techniques to be applied in real-life energy harvesting systems.

^a e-mail: telles@eng.uerj.br

^b e-mail: mardapereira@firjan.com.br

^c e-mail: americo.cunha@uerj.br (corresponding author)

^d e-mail: lisandro@uerj.br

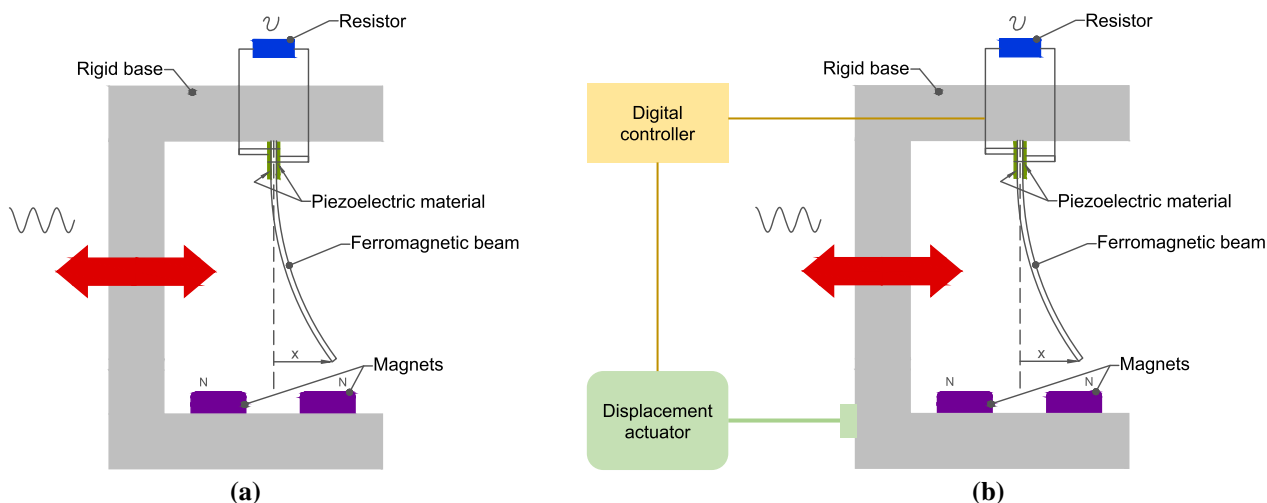


Fig. 1 Schematic representation of a typical piezoelectric vibration bistable energy harvester: **a** uncontrolled system, and **b** system with a digital controller mechanism attached

Seeking to fill this gap in the literature, and pave the way for an application of chaos control in a real-life energy harvesting system, this paper combines a digital controller with a displacement-based actuator to obtain an Extended Time-Delayed Feedback (ETDF) chaos control system suitable for laboratory implementations of energy harvesters under harmonic excitation. The underlying mathematical formulation is presented, and the new controller is tested on a bistable system.

2 Nonlinear dynamical system

The chaotic dynamics of the nonlinear bistable energy harvesting system shown in Fig. 1a can be controlled with an aid of a digital control system that performs the actuation on the system through a displacement transduction mechanism, as shown in the schematic representation in Fig. 1b. The dynamics of this controlled system can be modeled by the following dimensionless system of equations (see Ref. [25] for details)

$$\ddot{x} + 2\xi \dot{x} - \frac{1}{2}x(1-x^2) - \chi v = -u(t), \quad (1)$$

$$\dot{v} + \lambda v + \kappa \dot{x} = 0, \quad (2)$$

$$x(0) = x_0, \dot{x}(0) = \dot{x}_0, v(0) = v_0, \quad (3)$$

where $x(t)$ is the transverse displacement of the beam tip; $v(t)$ is the voltage across the resistor; $u(t)$ is the external excitation; t denotes the time; ξ is the damping factor; χ the electromechanical coupling coefficient in the mechanical equation; λ the inverse of the electrical characteristic time; κ the electromechanical coupling coefficient in the electrical equation; x_0 the beam tip initial displacement; \dot{x}_0 the beam tip initial velocity; and v_0 is the initial voltage across the circuit. When the system is not controlled, as in Fig. 1a, the external

excitation takes the form

$$u(t) = -f \cos(\Omega t), \quad (4)$$

where f is the amplitude of the inertial excitation imposed by the moving base, and Ω is the underlying excitation frequency. On the other hand, when the controller is activated, such as in Fig. 1b, the external forcing takes the format

$$u(t) = -f \cos(\Omega t) + u_c(t), \quad (5)$$

where $u_c(t)$ is the control force imposed by the actuator. Remember that all these quantities are in dimensionless format.

3 Digital controller for chaos

The control system employed in this work, which is based on a displacement transduction mechanism, is schematically illustrated through block diagrams in Fig. 2. The objective of this controller is to avoid chaotic responses, when the system is subject to harmonic excitation, by imposing a controlled displacement $b(t)$ which is calculated by the digital controller using the voltage $v(t)$ as a feedback signal since this is the easiest state to be observed.

Note in Fig. 2 that the A/D converter sample the tension with a sampling period T_s , and the D/A converter uses a Zero Order Holder (ZOH). The idea is to implement a control law using a digital version of the ETDF method [26–28], for which the control law is defined as

$$b(t) = K((1-Q)s_\tau(t) - v(t)), \quad (6)$$

where

$$s_\tau(t) = \sum_{j=1}^{\infty} Q^{j-1} v(t - j\tau). \quad (7)$$

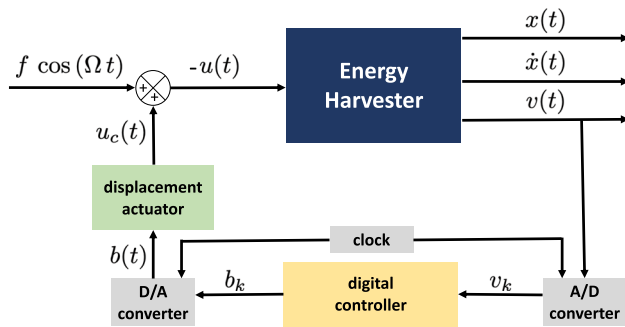


Fig. 2 Digital controller used to control the chaotic dynamics of the piezoelectric vibration bistable energy harvesting system

This control law can be discretized as

$$b_k = K [(1 - Q) s_k - v_k], \quad (8)$$

$$s_k = \sum_{j=1}^{\infty} Q^{j-1} v_{k-j}, \quad (9)$$

so that, after applying the Z-transform, the summation becomes

$$\begin{aligned} S_{\tau}(z) &= z^k V(z) \sum_{j=1}^{+\infty} Q^{j-1} z^{-j} \\ &= z^k V(z) \frac{z^{-1}}{1 - Q z^{-1}}, \end{aligned} \quad (10)$$

and, consequently, the digital version of the control law is written as

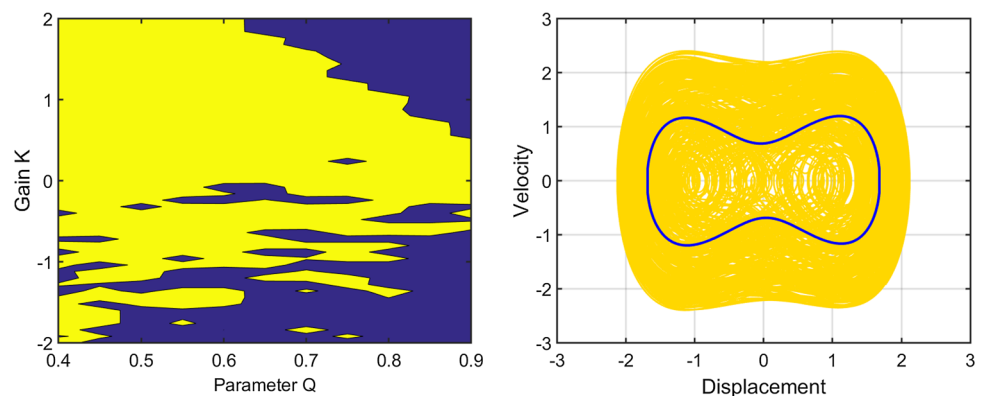
$$B(z) z^k = K z^k V(z) \left((1 - Q) \frac{z^{-1}}{1 - Q z^{-1}} - 1 \right). \quad (11)$$

Therefore, the ETDF can be digitally implemented using the following Transfer Function (TF)

$$B(z) = -K \frac{z - 1}{z - Q}, \quad (12)$$

where K and Q are tuning parameters.

Fig. 3 Contour map corresponding to the 0–1 test for chaos as function of the K and Q gains with $f = 0.7$ (left), as well as the chaotic trajectory and a typical regular orbit (right). Dark blue regions correspond to regular dynamics, while the regions in light yellow to chaos



The pole of this TF is located at $z_p = Q$ and the zero is located at $z_o = 1$. It can be concluded that it is necessary that $|Q| < 1$ to guarantee the stability of the controller, and the consequence is that the digital implementation of the ETDF is a lead compensator, since $z_o > z_p$. Therefore, this well-established compensator for linear control systems is proposed here to control the chaos.

At this point, it is worth mentioning that the reference [24] uses a Taylor expansion to represent the delayed operator in the proposed control loop, to then solve the resulting equations by a 4th order Runge–Kutta type integration scheme. In comparison with this approach, the digital filter-based control system proposed here is much simpler, which makes it more attractive to be implemented in the laboratory or the field.

To assess the efficiency of this control strategy over a time-window of length T , it is necessary to make a comparison between the RMS power recovered by the harvester

$$P_h = \sqrt{\frac{1}{T} \int_0^T \lambda v(t)^2 dt}, \quad (13)$$

with that which is consumed by the control system

$$P_c = \frac{1}{T} \int_0^T (\ddot{b}(t))^+ (\dot{b}(t))^+ dt, \quad (14)$$

where $(\cdot)^+$ denotes the positive part.

4 Results and discussion

The energy harvesting dynamical system is simulated using the parameters that correspond to the $145 \times 26 \times 0.26$ mm³ piezo-magneto-elastic steel beam analyzed by Stanton et al. [29]. In this harvester, the equivalent dimensionless parameters are $\xi = 0.01$, $\chi = 0.51$, $\kappa = 0.51$, $\lambda = 0.04$ and $\Omega = 0.8$. The initial condition adopted is $(x_0, \dot{x}_0, v_0) = (1, 0, 0)$. The value of excitation amplitude f is varied.

Initially, we observe the effect of the K and Q gains on the controller's operation with aid of the 0–1 test for chaos [30] shown in the left part of Fig. 3, where the dark blue regions correspond to regular dynamics,

Fig. 4 Comparison between test 0–1 for chaos as function of the amplitude f and frequency Ω of the external excitation, without control (left) and with control (right), assuming for the controlled case the gains $(K, Q) = (-1.9, 0.85)$

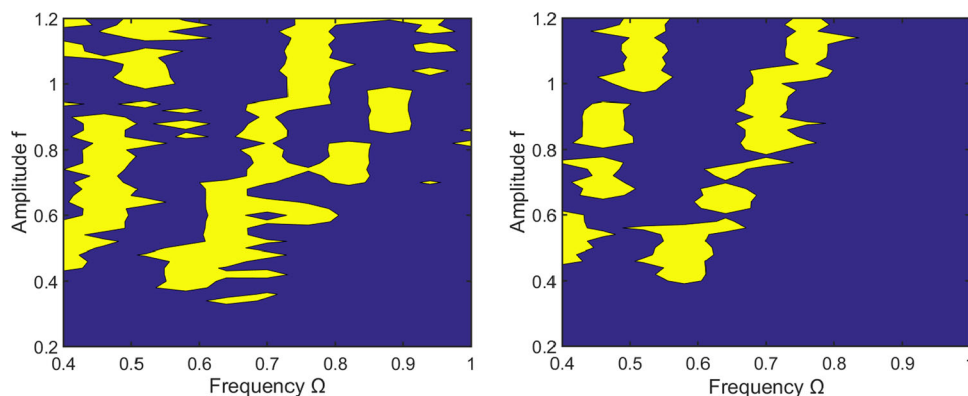


Fig. 5 **a** Chaotic voltage time series for the uncontrolled system; **b** Power spectrum of this chaotic voltage; **c** Regular voltage time series for the controlled system; **d** Power spectrum of this controlled voltage

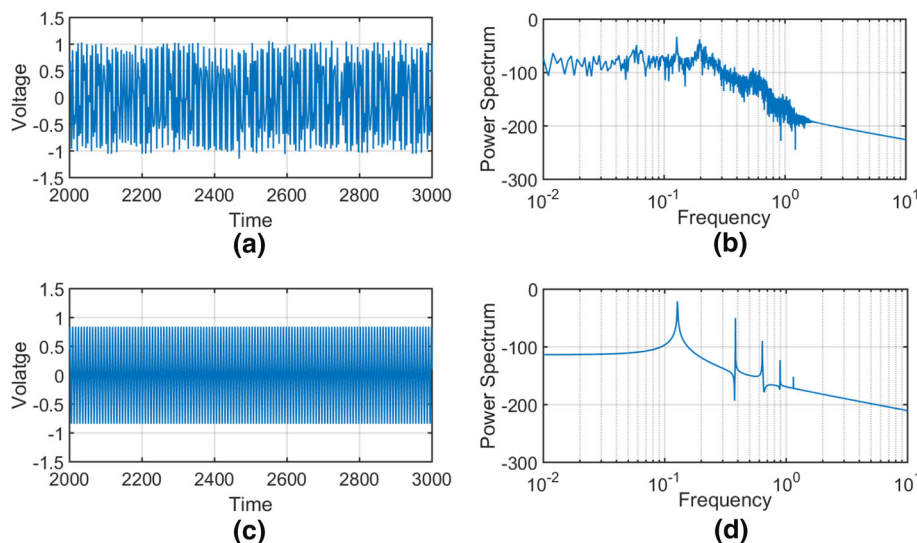
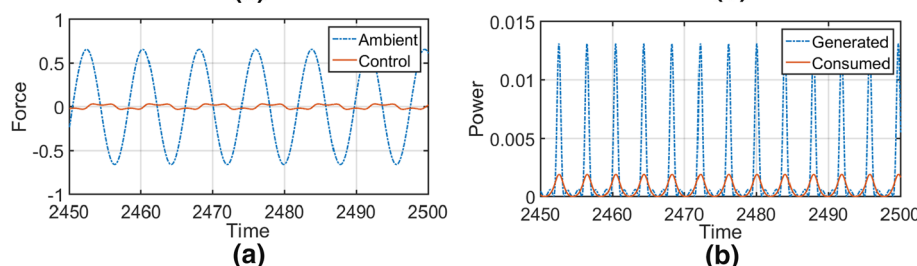


Fig. 6 **a** Ambient and control forces **b** Power generated by the harvester, and the power consumed by the controller



while the regions in light yellow to chaos. For reference, the chaotic trajectory and a (typical) regular period 1 orbit are shown on the right. It is clear that the effective functioning of the control strategy strongly depends on a good choice for the pair (K, Q) .

The optimal choice for these gains can be done, for instance, employing the cross-entropy method for optimization [31], but due to space limitation this issue is not addressed here (it will be the subject of a future work). Instead, let's focus on showing that, even without optimizing the gains, the proposed chaos control strategy is quite effective. See Fig. 4, which compares two diagrams obtained with test 0–1 as function of the amplitude f and frequency Ω of the external excitation, without control (left) and with control (right), assuming for the controlled case the gains $(K, Q) = (-1.9, 0.85)$. It is quite clear that control substantially

reduces the occurrence of chaos, once the light yellow region is smaller in the right map.

Figure 5 shows the voltage across the resistor for both, uncontrolled and controlled systems, as well as the corresponding power spectrum (obtained with steady-state part of the series). This result makes it very clear that the digital controller used is capable of regulating a chaotic voltage signal to facilitate its use, note that the spectrum changes from a continuum of frequencies to a signal with a few frequencies.

Finally, Fig. 6a shows the excitation force compared to the transducer force. The control signal amplitude is small with respect to ambient vibration, which translates into a low energy cost for the digital controller, as shown in Fig. 6b, which compares generated and consumed power. The RMS value of the consumed power is just 11% of the generated power. Depending on the orbit where the system is stabilized, substantial power

gains may or may not occur (already including rectification costs). But even with no power gain, the regularization of a chaotic orbit favors the efficiency of the energy recovery process by reducing the battery charging time [20].

5 Final remarks

This work presented the design of an extended time-delay feedback digital controller for the chaotic dynamics of a bistable energy harvester. This digital implementation seems to be a promising method to be implemented in chaos control, since it is an easy task using digital filters only. The results show that many orbits can be controlled, depending on the value of Q and the suppression of the chaos depends on K . The remaining problem is to establish the best values of K and Q , what can be done with aid of optimization [31] and sensitivity analysis [32] techniques. Furthermore, extending this formalism to a situation of non-harmonic excitation is an interesting line for future work. The simulations reported here used the computational package STONEHENGE—Suite for Nonlinear Analysis of Energy Harvesting Systems [33], which available for free and can be used to reproduce the reported results.

Acknowledgements This research received financial support from the Brazilian agencies Coordenação de Aperfeiçoamento de Pessoal de Nível Superior - Brasil (CAPES) - Finance Code 001, and the Carlos Chagas Filho Research Foundation of Rio de Janeiro State (FAPERJ) under the following grants: 211.304/2015, 210.021/2018, 210.167/2019, 211.037/2019 and 201.294/2021.

References

1. A. Erturk, D.J. Inman, *Piezoelectric Energy Harvesting*, 1st edn. (Wiley, New Jersey, 2011)
2. S. Beeby, Z. Cao, A. Almussallam, in *Multidisciplinary Know-How for Smart-Textiles Developers*, ed. by T. Kirstein (Woodhead Publishing, 2013), pp. 306–328. <https://doi.org/10.1533/9780857093530.2.306>
3. F. Cottone, H. Vocca, L. Gammaitoni, *Phys. Rev. Lett.* **102**, 080601 (2009). <https://doi.org/10.1103/PhysRevLett.102.080601>
4. A. Erturk, J. Hoffmann, D.J. Inman, *Appl. Phys. Lett.* **94**, 254102 (2009). <https://doi.org/10.1063/1.3159815>
5. A. Erturk, D.J. Inman, *J. Sound Vib.* **330**, 2339 (2011). <https://doi.org/10.1016/j.jsv.2010.11.018>
6. R.L. Harne, K.W. Wang, *Smart Mater. Struct.* **22**(2), 023001 (2013). <https://doi.org/10.1088/0964-1726/22/2/023001>
7. S. Zhou, J. Cao, D.J. Inman, J. Lin, S. Liu, Z. Wang, *Appl. Energy* **133**, 33 (2014). <https://doi.org/10.1016/j.apenergy.2014.07.077>
8. V.G. Lopes, J.V.L.L. Peterson, A. Cunha Jr, in *24th ABCM International Congress of Mechanical Engineering* (Curitiba, Brazil, 2017)
9. V.G. Lopes, J.V.L.L. Peterson, A. Cunha Jr, in *XXXVII Congresso Nacional de Matemática Aplicada e Computacional* (São José dos Campos, Brazil, 2017)
10. V. Lopes, J. Peterson, A. Cunha Jr., *Topics in Nonlinear Mechanics and Physics*, vol. 228 (Springer, Singapore, 2019), pp. 71–88
11. A. Erturk, D. Inman, *J. Intell. Mater. Syst. Struct.* **19**(11), 1311 (2008). <https://doi.org/10.1177/1045389X07085639>
12. A. Erturk, D.J. Inman, *J. Vib. Acoust.* **130**(4), 041002 (2008). <https://doi.org/10.1115/1.2890402>
13. A. Erturk, D.J. Inman, *Smart Mater. Struct.* **17**(6), 065016 (2008). <https://doi.org/10.1088/0964-1726/17/6/065016>
14. A. Erturk, D.J. Inman, *Smart Mater. Struct.* **18**(2), 025009 (2009). <https://doi.org/10.1088/0964-1726/18/2/025009>
15. O. Bilgen, Y. Wang, D.J. Inman, *Mech. Syst. Signal Process.* **27**, 763 (2012). <https://doi.org/10.1016/j.ymssp.2011.09.002>
16. M. Lumentut, I. Howard, *Mech. Syst. Signal Process.* **36**(1), 66 (2013). <https://doi.org/10.1016/j.ymssp.2011.07.010>. Piezoelectric Technology
17. S.R. Anton, A. Erturk, D.J. Inman, *J. Aircr.* **49**(1), 292 (2012). <https://doi.org/10.2514/1.C031542>
18. Y. Wang, D.J. Inman, *J. Compos. Mater.* **47**(1), 125 (2013). <https://doi.org/10.1177/0021998312448677>
19. Y. Wang, Z. Yang, P. Li, D. Cao, W. Huang, D.J. Inman, *Nano Energy* **75**, 104853 (2020). <https://doi.org/10.1016/j.nanoen.2020.104853>
20. M.F. Daqaq, R.S. Crespo, S. Ha, *Nonlinear Dyn.* **99**, 1525 (2020). <https://doi.org/10.1007/s11071-019-05372-0>
21. E. Ott, C. Grebogi, J.A. Yorke, *Phys. Rev. Lett.* **64**, 1196 (1990). <https://doi.org/10.1103/PhysRevLett.64.1196>
22. A. Kumar, S.F. Ali, A. Arockiarajan, *IFAC-PapersOnLine. 4th IFAC Conference on Advances in Control and Optimization of Dynamical Systems ACODS 2016* **49**(1), 35 (2016). <https://doi.org/10.1016/j.ifacol.2016.03.025>
23. L. de la Roca, J.V.L.L. Peterson, M. P. A. Cunha Jr, in *25th International Congress of Mechanical Engineering* (Uberlândia, Brazil, 2019)
24. W.O.V. Barbosa, A.S. De Paula, M.A. Savi, D.J. Inman, *Eur. Phys. J. Spec. Top.* **224**, 2787 (2015). <https://doi.org/10.1140/epjst/e2015-02589-1>
25. M.F. Daqaq, R. Masana, A. Erturk, D. Dane Quinn, *Appl. Mech. Rev.* **66**(4) (2014). <https://doi.org/10.1115/1.4026278>
26. K. Pyragas, *Phys. Lett. A* **206**(5), 323 (1995). [https://doi.org/10.1016/0375-9601\(95\)00654-L](https://doi.org/10.1016/0375-9601(95)00654-L)
27. M. Bleich, J. Socolar, *Phys. Lett. A* **210**(1), 87 (1996). [https://doi.org/10.1016/0375-9601\(95\)00827-6](https://doi.org/10.1016/0375-9601(95)00827-6)
28. A.S. de Paula, M.A. Savi, *Int. J. Non-Linear Mech.* **46**(8), 1076 (2011). <https://doi.org/10.1016/j.ijnonlinmec.2011.04.031>
29. S.C. Stanton, B.A. Owens, B.P. Mann, *J. Sound Vib.* **331**(15), 3617 (2012). <https://doi.org/10.1016/j.jsv.2012.03.012>
30. G.A. Gottwald, I. Melbourne, in *Chaos Detection and Predictability, Springer Lecture Notes in Physics*, vol. 915, ed. by C. Skokos, G.A. Gottwald,

- J. Laskar (Springer, 2016). <https://doi.org/10.1007/978-3-662-48410-4>
31. A. Cunha Jr., *Nonlinear Dyn.* **103**, 137 (2021). <https://doi.org/10.1007/s11071-020-06109-0>
32. J.P. Norenberg, A. Cunha Jr., S. da Silva, P.S. Varoto. Global sensitivity analysis of (a)symmetric energy harvesters (2021)
33. J.P. Norenberg, J.V. Peterson, V.G. Lopes, R. Luo, L. de la Roca, M. Pereira, J.G. Telles Ribeiro, A. Cunha, *Softw. Impacts* **10**, 100161 (2021). <https://doi.org/10.1016/j.simpa.2021.100161>